DETECTION OF 3D SYMMETRY AXIS FROM FRAGMENTS OF A BROKEN POTTERY BOWL

Fenghui YAO[+], *Guifeng SHAO*[++]

[+]Shimane University, 1060 Nishikawatsu-machi, Matsue-shi, Japan 6908504
[++]Seinan Gakuin University, 6-2-92 Nishijin, Sawara-ku, Fukuoka, Japan 8140002

ABSTRACT

This paper relates a method to detect three-dimensional (3D) symmetry axis from the fragment of a broken pottery bowl, which is symmetric in the original status (that is, before broken). Firstly, the fragment is extracted from the range image by applying a bias processing, and its contour is detected. Next, the corner points of the 3D fragment are extracted from its contour. Then, the contour of the 3D fragment is separated into 3D curve segments at the corner points, and the *partial mouth-edge* is determined by reasoning its center coordinates. Finally, by shrinking the range image, a series of partial curves which are in parallel with the partial mouth-edge, is obtained. The symmetry axis is thought as a line passing through the center points of these partial curves, in 3D space. We tested this method by using the real-world range data. The experiment results are satisfactory.

1. INTRODUCTION

As pointed by Weyl, symmetry is one idea by which man through the ages has tried to comprehend and create order, beauty, and perfection [1]. It plays a significant role in the analysis and understanding of form by humans and it is recognized as a necessary component of the successful intelligent, autonomous system based on the principles of computer vision, pattern recognition, and decision making. Up to present, the studies about symmetry focuses on the symmetry detection based on 3D data of the complete 3D object [1] [2]. On the other hand, few work has been conducted toward the symmetry identification of the fragment that is originally a part of a complete 3D symmetry object. This need arises in the archaeological application area where the problem is to reconstruct a complete object from its fragments (or parts). Because many artificial 3D objects such as pottery bowls, dishes, vases and so on, are made based on the rotation-manufacturing, their symmetry is represented by the rotation axis. Therefore, for a broken pottery bowl, if its rotation axis can be detected from its fragment, the original shape can be reconstructed easily by translating and rotating the fragments so that their axes overlap on the same line and then performing rotation and matching operations. For the pottery bowl and vase, the symmetry axis is the same with that of rotation axis.

In the present paper, we propose a method for reasoning the symmetry axis from the fragment of a broken pottery bowl. In this method, the fragment in 3D space is thought of as a thin surface that is represented by the range image. The fragment is extracted from the range image by applying a bias processing, and its contour is detected. Next, the corner points of the 3D fragment are extracted from its contour. Then, the contour of the 3D fragment is separated into 3D curve segments at the corner points, and the partial mouth-edge is determined by reasoning its center coordinates. Finally, by shrinking the range image, a series of partial curves which are in parallel with the partial mouth-edge, is obtained. The symmetry axis is thought as a line passing through the center points of these partial curves, in 3D space. Details are given in the following.

2. BOWL BROKEN PROCESS AND POTTERY FRAGMENT SHAPE FEATURES

The problem we deal with in this paper can be described as follows.

[*Problem*] For a fragment, it is known to be a part of a symmetric bowl, *W*, and its 3D shape is represented by 3D point set, S_i, find the symmetry axis of *W* from S_i.

In other words, this problem is to try to find the symmetry axis of a complete bowl, *W*, from incomplete 3D points, S_i. Before solving this problem, let us see how the pottery fragment is generated and what features the pottery fragment has. Fig.1 (a) shows a pottery bowl in good status. It has a perfect *mouth-edge* and a perfect *bottom-edge*, shown by red circle and green circle respectively, and a symmetry axis by blue. If it falls down to the ground or collides with harder objects such as stone or other bowls, it will be broken into several fragments. Fig. 1 (b) shows its fragments after being broken, in which the inner surfaces of them are upward. These fragments have following features.

They can be roughly classified into two categories, the *boundary fragments* and *interior fragments*. Boundary

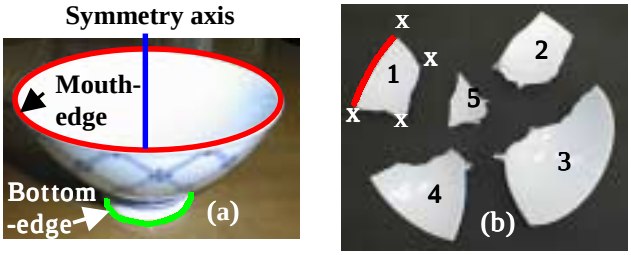

Fig. 1 (a) is a pottery bowl in good status, (b) shows fragments of the bowl in (a) after being broken.

fragments are the fragments that contain, more or less, a part of the mouth-edge. Interior fragments are the fragments that do not contain any part of mouth-edge at all. Usually, the number of boundary fragments is bigger than that of interior fragment. The fragments labeled 1, 2, 3 and 4 in Fig. 1 (b) are boundary fragments, and 5 is the interior fragment.

(i) If we focus on the edge (contour) of the fragment, it can be separated into *partial edges* at the corner points (see the points marked "x" on the fragment labeled 1 in Fig.1 (b)). For the boundary fragment, one of the partial edge is corresponding to a part of the mouth-edge, that is called the *partial mouth-edge* (e.g., the curve segment marked by the red line on the fragment labeled 1 in Fig.1 (b)), others are *generated edges*. Note that the partial mouth-edge exists in the bowl in good status before being broken, and for the interior fragments, all partial edges are generated edges.

(ii) The partial mouth-edge is a very smooth curve, more specifically, it is a part of a circumference (or ellipse) in 3D space.

The above features play important roles in symmetry axis detection in the later sections. Here we limit to discuss the symmetry axis detection from the boundary fragments. And if no special explanation, the size of the fragment is large enough that the symmetry axis does exist in that fragment. Note that if the size of a fragment becomes very small, the surface of the fragment is near to a plane, in this case the symmetry axis will disappear.

3. PROPOSED ALGORITHM

Our algorithm to detect the symmetry axis from fragment can be formulated in four steps: fragment extraction, corner point detection, partial mouth-edge identification and symmetry axis detection. These steps are explained in greater detail in the following.

3.1. 3D Fragment Edge Extraction

Let $F_i(x, y)$ represent the range data of the fragment F_i, output by the laser range finder, and $B_i(x, y)$ the contour of F_i, where x and y is the horizontal and vertical coordinates, respectively. The value of $F_i(x, y)$ lies in the range from -90 mm to +90 mm to the reference plane. The reference plane is 45 cm under the laser detector head. The positive range data means that the target is over the reference plane, and the negative under. The contour, $B_i(x, y)$, is what we want to determine from the range data, $F_i(x, y)$. The algorithm is as follows. Note that the Cartesian coordinate system is employed in the following if no specific declaration.

(1) Bias processing

For the range data, $F_i(x, y)$, if the value at point (x,y) is less than T_{bias}, the output is set to 0, otherwise the output is set to $F_i(x, y) - T_{bias}$, where T_{bias} is the threshold value predetermined experimentally. From here on, if no specific explanation, $F_i(x, y)$ means the range data after the bias processing.

(2) Edge detection

$F_i(x, y)$ is projected to the xy-plane to obtained its silhouette. Let $F'_i(x, y)$ represent the silhouette of $F_i(x, y)$ to xy-plane, and $B'_i(x(s),y(s))$ the boundary curve of $F'_i(x, y)$, where s is a path-length variable along the curve. $F'_i(x, y)$ is generated in such a way that $F'_i(x, y)$ is set to 255 if $F_i(x, y) > 0$, otherwise to 0. $B'_i(x(s),y(s))$ is detected by applying the boundary curve tracing algorithm [4]. Here and after, $B'_i(x(s),y(s))$ is simply written as $B'_i(x,y)$ if no confusion. $B'_i(x,y)$ is a closed digital curve in 2D space. The value of $B'_i(x,y)$ is fixed at 255. $B'_i(x,y)$ is projected back to the range data $F_i(x, y)$, then we obtain the 3D boundary curve, $B_i(x, y)$, by setting the value of $B_i(x, y)$ to the range data, $F_i(x, y)$, at point (x,y). Note that x- and y-coordinates in $B_i(x, y)$ are corresponding to x- and y-coordinates in $B'_i(x, y)$.

3.2. Fragment Corner Point Detection

Our strategy to detect the fragment corner points is as follows: Firstly, the dominant points of 2D boundary curve, $B'_i(x,y)$, are extracted. Then, corner points of the silhouette image, $F'_i(x,y)$, are detected by applying the filtering operation to the dominant points of $B'_i(x,y)$. The corner points of $B'_i(x,y)$ are projected back to 3D space to get the corner points of $B_i(x, y)$.

(1) 2D dominant point detection

There have been many attempts to detect dominant points [5] [6]. Among the proposed methods, the one developed by Rattarangsi and Chin, based on multiple-scale curvature, is reliable and robust with respect to noise. Therefore, we employ this method to detect the dominant points. Details are referred to [5].

(2) Corner point detection

The 2D corner points are the special 2D dominant points

in which the interior junction or boundary junction exists. A *triradial* junction is the junction of three fragments. A *quadradial* junction joins four fragments. 2D corner point detection is a filtering operation. For *k*-th 2D dominant point (*k* = 0, 1, ..., *N*-1), if its interior angle is greater than the threshold value $T_{interior}$, it is discarded, where *N* is the total number of the dominant points. After this filtering, the left dominant points are considered as the 2D corner points. Note that the interior angle at *k*-th dominant point is the angle formed by three consecutive dominant points, *i.e.*, (*k*-1)-th, *k*-th and (*k*+1)-th dominant point (modulo *N*). By projecting the 2D corner points to 3D space, we obtain 3D corner points of $B_i(x,y)$. Let us denote 3D corner points by $S_{B_i} = \{ C_i^0, C_i^1, ..., C_i^{N'-1} \}$, in which the *x*- and *y*-coordinates are corresponding to those of 2D corner points, the value of C_i^k (k = 0, 1, ..., N'-1) is set to the range data, $F_i(x,y)$, at the boundary point (x, y).

3.3. PARTIAL MOUTH-EDGE IDENTIFICATION

By taking the 3D corner points, $\{ C_i^0, C_i^1, ..., C_i^{N'-1} \}$, as the separation point, the 3D boundary curve, $B_i(x, y)$, is separated into a set of 3D partial curves by tracing the corner points clockwise. Let $E_i^{m,m+1}$ express *m*-th partial curve in which *m* means initial corner point and *m+1* the terminal, and $L_i^{m,m+1}$ express the length of *m*-th partial curve, that is the total number of the boundary points on *m*-th partial curve. The partial curve set is expressed as $S_{E_i} = \{ E_i^{01}, E_i^{12}, ..., E_i^{N'-2,N'-1}, E_i^{N'-1,0} \}$ (modulo N'), and the partial curve length set of the corresponding partial curve set is denoted as $S_{L_i} = \{ L_i^{01}, L_i^{12}, ..., L_i^{N'-2,N'-1}, L_i^{N'-1,0} \}$ (modulo N'),.

The partial mouth-edge has the following properties. (i) It is a part of a circumference (or ellipse in general) in 3D space because the fragment is a part of a bowl; (ii) All points on the partial mouth-edge lie on the same plane in 3D space. The partial mouth-edge recognition is based on identifying its center coordinates and radius. Details are shown below.

For the *m*-th partial curve, $E_i^{m,m+1}$, it is further separated into three curve segments, $E_i^{m,m+K-1}$, $E_i^{m+K,m+2K-1}$ and $E_i^{m+2K,m+1}$, where *m*+*a* (*a* = *K*-1, *K*, 2*K*-1, 2*K*) means *a*-th boundary point from *m*-th corner point, and $K = L_i^{m,m+1} / 3$. Now taking one point from each

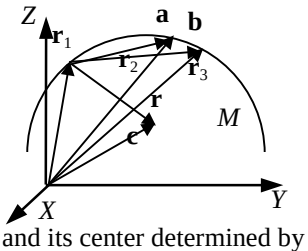

Fig. 2 Circle and its center determined by three points.

of these three curve segments, *i.e.*, $P_1(\mathbf{r}_1) \in E_i^{m,m+K-1}$, $P_2(\mathbf{r}_2) \in E_i^{m+K,m+2K-1}$ and $P_3(\mathbf{r}_3) \in E_i^{m+2K,m+1}$, let us check whether these three points lie on the circumference of the same circle in 3D space or not. If they do, $P_1(\mathbf{r}_1)$, $P_2(\mathbf{r}_2)$, $P_3(\mathbf{r}_3)$ and the center C(**c**) of the circle will lie on the same plane *M* in 3D space. As shown in Fig. 2, let **a** = $\mathbf{r}_2$- $\mathbf{r}_1$ and **b** = $\mathbf{r}_3$- $\mathbf{r}_1$, the normal vector of *M* is given by **a**× **b**. and let **r** = **c**- $\mathbf{r}_1$, then **r**(**a**× **b**) = 0. Moreover, the plane M_1 passing the center C(**c**) and the middle point of $\overline{\mathbf{r}_1\mathbf{r}_2}$ and perpendicular to $\overline{\mathbf{r}_1\mathbf{r}_2}$ is expressed as (**r**-**a**/2)**a** = 0. Similarly, the plane M_2 passing the center C(**c**) and the middle point of $\overline{\mathbf{r}_1\mathbf{r}_3}$ and perpendicular to $\overline{\mathbf{r}_1\mathbf{r}_3}$ is given by (**r**-**b**/2)**b** = 0. The center C(**c**) is the cross point of three planes, *M*, M_1 and M_2. It is determined by

$$\mathbf{c} = \mathbf{r_1} + \frac{\mathbf{b}^2(\mathbf{a}^2 - \mathbf{ab})\mathbf{a} + \mathbf{a}^2(\mathbf{b}^2 - \mathbf{ab})\mathbf{b}}{2|\mathbf{a}\times\mathbf{b}|^2}. \qquad (1)$$

The radius of this circle is given by

$$R = \left(\frac{|\mathbf{a}|^2|\mathbf{b}|^2(\mathbf{a}-\mathbf{b})^2}{4|\mathbf{a}\times\mathbf{b}|^2} \right)^{1/2}. \qquad (2)$$

Note that the bold lower case letters are vectors in 3D space.

By taking all triple points from the beginnings of $E_i^{m,m+K-1}$, $E_i^{m+K,m+2K-1}$ and $E_i^{m+2K,m+1}$, sequentially, their center coordinates and the radius of the circle determined by the triple points are calculated. The standard deviations of the radius and center coordinates (*x*-, *y*- and *z*-coordinate) are calculated. If the total sum of these standard deviations is smaller than a predetermined threshold value $T_{mouth\text{-}edge}$, $E_i^{m,m+1}$ is considered as the partial mouth-edge.

The plane *M* is reasoned according to least-square method (LSM) as below. Let *M* be represented by

$$M: Ax + By + Cz + D = 0. \qquad (3)$$

Because *A*, *B*, *C* and *D* are not linearly independent, they cannot be determined uniquely. The equation (3) can be rewritten as

$$M: D(ax + by + cz + 1) = 0. \quad (4)$$

By setting D at constant value beforehand, a, b and c are obtained by solving the following equation.

$$\mathbf{Ax} = \mathbf{b} \quad (5)$$

where $\mathbf{A}=\begin{pmatrix} \sum x_i^2 & \sum x_i y_i & \sum x_i z_i \\ \sum x_i y_i & \sum y_i^2 & \sum y_i z_i \\ \sum x_i z_i & \sum y_i z_i & \sum z_i^2 \end{pmatrix}$, $\mathbf{x} = (a, b, c)^{\mathrm{T}}$ and $\mathbf{b} = (-1)(\Sigma x_i, \Sigma y_i, \Sigma z_i)^{\mathrm{T}}$, (x_i, y_i, z_i) is the point on $E_i^{m,m+1}$. The normal vector of M is given by

$$\mathbf{n}_i = (a, b, c)\frac{1}{\sqrt{a^2 + b^2 + c^2}}. \quad (6)$$

3.4 SYMMETRY AXIS DETECTION

The symmetry axis is a line in 3D space. Let L_{sym} express the symmetry axis, it is obtained as follows. The silhouette, $F'_i(x, y)$, is shrunk, and the processing described in section 3.1, 3.2 and 3.3 is repeated. This operation is iterated until the area of $F'_i(x, y)$ becomes smaller than a predetermined threshold value T_{silh}. Then we obtained a series of center points and normal vector according to equation (1) to (6). Suppose the number of center points is N, the direction vector of L_{sym} is given by

$$\mathbf{n}_L = (m, n, p) = \frac{1}{N}\sum \mathbf{n}_i \quad (7)$$

and the symmetry axis is determined as

$$L_{\mathrm{sym}}: \quad \frac{x-\alpha}{m} = \frac{x-\beta}{n} = \frac{x-\gamma}{p} \quad (8)$$

where $\alpha = \frac{1}{N}\sum x_{ci}$, $\beta = \frac{1}{N}\sum y_{ci}$, $\gamma = \frac{1}{N}\sum z_{ci}$ and (x_{ci}, y_{ci}, z_{ci}) is i-th center point.

The pitch and yaw angle of L_{sym} are calculated, respectively, as below,

$$\theta = \cos^{-1}\frac{m}{\sqrt{m^2 + p^2}}, \quad \varphi = \cos^{-1}\frac{n}{\sqrt{n^2 + p^2}}. \quad (9)$$

4. EXPERIMENT RESULTS

The algorithm was coded on Windows platform and the programming language is MS-VC++ ver 6.0. Values for T_{bias}, T_{interior}, $T_{\mathrm{mouth\text{-}edge}}$ and T_{silh} are 36 mm, 165°, 60 and 150 dots, respectively. Fig.3 (a) shows the picture of a piece of fragment of a broken pottery bowl, (b) shows its range image. The corner points are shown in (c). The partial mouth-edges and center points are detected from shrunk range image. The pitch and yaw angle of the symmetry axis are 14.4° and 34°, respectively. The rotated fragment with the mouth-edge upward is shown in (d).

We also tested this algorithm with other real-world range images. The algorithm works well.

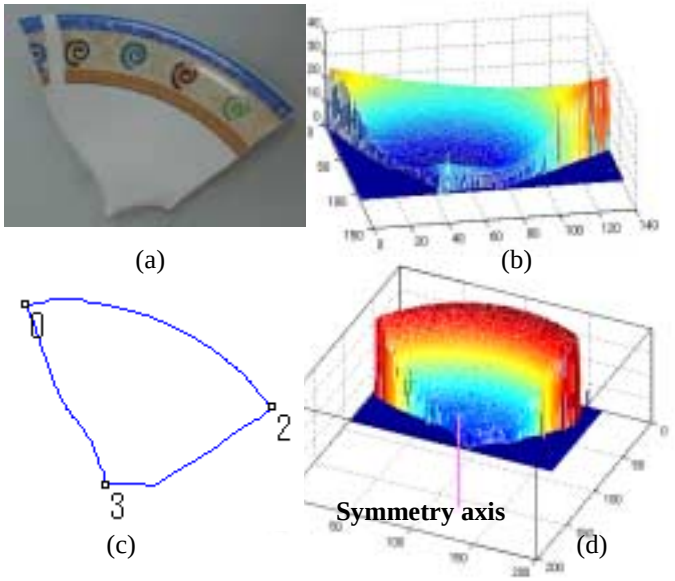

Fig. 3 (a) Photo of a piece of fragment; (b) Range image of the fragment in (a); (c) Detected corner points; (d) symmetry axis after being rotated.

5. CONCLUSIONS

This paper related a method to detect the symmetry axis from the fragment of a broken pottery bowl. The algorithm consists of fragment edge extraction, corner point detection, partial mouth-edge identification and symmetry axis detection. We tested the algorithm with the real-world 3D range images. The experiment results are satisfactory. This algorithm can be applied in the archaeological area where the problem is to reconstruct a complete object from its fragments. This will be done in the future.

REFERENCES

[1] H. Weyl, "Symmetry," in H. Weyl gesammelte Abhandlungen (K. Chandrasekharan, Heraus.), Bd. III, pp.592-610, Springer, Berlin, 1968.

[2] P. Minovic, "Symmetry Identification of a 3-D Object Represented by Octree, " *IEEE Trans. Patt. Anal. & Mach. Intell.*, Vol. 15, No.5, pp.507-514, 1993.

[3] P. Eades, "Symmetry Finding Algorithm," in: G. T. Toussaint, Ed., *Computational Morphology*, Amsterdam, North-Holland, pp.41-51, 1988.

[4] J. Hasegawa, et al, ed., "Image Processing on Personal Computer," Gijyutsu-Hyoron Co., Ltd., Toko, 1986.

[5] A. Rattarangsi and R. T. Chin, "Scale-based detection of corners of planar curves," *IEEE Trans. Patt. Anal. Mach. Intell.*, vol. PAMI-14, No. 4, pp. 432-449, 1992.